Talanta 222 (2021) 121536

Contents lists available at ScienceDirect

Talanta

journal homepage: www.elsevier.com/locate/talanta

Enzyme-free electrochemical biosensor based on amplification of proximity-dependent surface hybridization chain reaction for ultrasensitive mRNA detection

Yu-Hong Cheng [a], Si-Jia Liu [b,*], Jian-Hui Jiang [a,**]

[a] State Key Laboratory of Chemo/Biosensing and Chemometrics, College of Chemistry and Chemical Engineering, Hunan University, Changsha, 410082, PR China
[b] Guangxi Collaborative Innovation Center for Biomedicine, Guangxi Key Laboratory of Regenerative Medicine, Key Laboratory of Longevity and Aging-related Diseases of Chinese Ministry of Education, School of Basic Medical Sciences, Center for Translational Medicine, Guangxi Medical University, Nanning, 530021, PR China

ARTICLE INFO

Keywords:
Electrochemical biosensor
Hybridization chain reaction
Survivin mRNA
Proximity-dependent surface hybridization
Ferrocene-tagged

ABSTRACT

The ability to recognize mRNA with high efficiency in cells would greatly facilitate the elucidation of mRNA-mediated cellular cascades and their disease associations. However, most traditional electrochemical strategies targeting nucleotides are always confronted with cumbersome interface operation and washing procedures, as well as the high cost of labeling and the strict reaction conditions of tool enzymes, limiting their potential applications. To address these issues, herein we reported, for the first time, a simple label-free, isothermal, non-enzymatic, and ultrasensitive homogeneous electrochemical biosensor based on autonomous proximity-dependent surface hybridization chain reaction (HCR), for sensitive signal amplification and highly specific detection of target *survivin* mRNA with a detection limit of 3 fM. The target triggers hybridization chain reaction and mRNA-fueled surface hybridization of ferrocene-tagged metastable DNA hairpin probes on proximity-dependent surface hybridization, resulting in the formation of multiple long-range duplex DNA chains which are immobilized onto the gold electrodes with a substantially stable ferrocene-mediated redox current. Thus, a significant electrochemical signal increase is observed dependent on the concentration of the target RNA, with a very low detection limit. Mo-reover, this molecular biosensor also exhibits excellent specificity to distinguish even single base mismatched, with strong reliability. The developed biosensor provides a novel promising tool for ultra-sensitive and selective detection, and it has great potential to be applied in mRNA-related biochemical research and clinical cancer diagnostics in more detail.

1. Introduction

Quantitative analysis of messenger RNA (mRNA) variants expression with high accuracy in cells would greatly facilitate the elucidation of mRNA-mediated cellular cascades and their disease associations [1,2]. Researchers have proved that specific tumor-related mRNAs are useful indicators during tumorigenesis and their expression level is highly related to the progression and/or prognosis of the indicated cancer [3,4]. Thus, specific identification and detection of tumor-related mRNA hold a great promise for early diagnosis and treatment against cancer. Although with individual advantages, traditional detection methods, such as Northern blot analysis [5], *in situ* hybridization (ISH) [6], ribonuclease protection assay (RPA) [7], and cDNA-microarray hybridization with optical or electrochemical readouts [8,9], have obvious limited sensitivity in detecting mRNA at the cellular level and regulation with a detection limit at the nanomolar level. This shortcoming is largely due to the lack of signal amplification mechanisms in these methods. Recently, the most widely-used thermal-cycling protocol for the analysis of specific mRNA expression levels is the reverse transcription polymerase chain reaction (RT-PCR) assay which through the synthesis of cDNA from a cellular mRNA [10,11]. As the increase of the product amount is acquired by repeated thermal cycling in an exponential way, PCR-based amplification assay is time-consuming and sometimes non-specific that depends on both thermo-stable enzymes and the laboratory setting. Some other amplification assays such as rolling circle amplification [12–14], enzyme-assisted amplification

* Corresponding author.
** Corresponding author.
E-mail addresses: heming_liu@163.com (S.-J. Liu), jianhuijiang@hnu.edu.cn (J.-H. Jiang).

https://doi.org/10.1016/j.talanta.2020.121536
Received 13 June 2020; Received in revised form 4 August 2020; Accepted 8 August 2020
Available online 25 August 2020
0039-9140/© 2020 Elsevier B.V. All rights reserved.

[15–18], and strand displacement amplification [19–21], are enzyme-based with increased complexity. Hybridization chain reaction (HCR) is a kinetics-controlled reaction in which a cascade of hybridization events between two species of metastable DNA hairpin probes is triggered to form a long dsDNA structure. In contrast to the traditional assays, HCR amplification offers very high sensitivity and selectivity for biological detection. Actually, HCR is relatively simple and can process under mild experimental conditions, thus representing a promising enzyme-free isothermal signal amplification technique with easy operation and low cost. Now it has been well developed for simple-to-use and sensitive amplified detection of DNA, microRNA, small molecules, proteins, and other biological signals, providing a useful nanosensor platform in low-abundance biomarker discovery and regulation for cell biology and diagnostics [22–30].

However, novel electrochemical biosensor with high sensitivity and low cost, coupled with their inherent miniaturization and independence of sample turbidity, will make themselves of great potential in large-scale genetic diagnostics and testing. With reversibility and synthetical versatility, Ferrocene (Fc)-derivative redox has been used to promote the detection performance as useful probes in electrochemical nucleic acid detection [31–33], as they can well guarantee the hybridization efficiency and interaction of nucleic acids with the related analytes. For this reason, for the first time, we hereby develop a novel electrochemical sensor by integrating proximity ligation strategy with HCR amplification reaction to realize highly specific detection assay for target RNA. By this new method, the proposed biosensors depend on the initial hybridization of segments of a pair of H1 probes and its connector H2 probes, followed by a released Fc-labeled tail sequence of H1 probe, the short thioled surface-tethered probes close proximity to hybridize together subsequently. The key strategy challenge for this biosensor relies on simultaneous recognition of a certain target by a pair of affinity probes, which releases the oligonucleotide tails of the bound probes into close proximity for the induction of ligation or hybridization [31,34–37]. One of hairpin probes has a 3′-ferrocene-labeled eight-nucleotide tail sequence that is complementary to the surface-tethered DNA strands with a predesigned low melting temperature (usually <20 °C). In the absence of the HCR amplification reaction, the ferrocene-labeled tail sequence does not associate with the surface-tethered strands because the complementary fragment is too short to promote effective annealing. When the hairpin monomers is triggered by initiator to form a long dsDNA structure, the tail sequences are brought into close proximity with their local concentration increased substantially to allow ferrocene-labeled tail sequences to hybridize together with the surface-tethered DNA strands. Then the ferrocene labels of the tail sequence are drawn close to the electrode surface, producing a readily detectable redox current. Herein, we choose survivin mRNA, a well-known biomarker in multiple kinds of cancer tissues, as a target RNA to initialize the hybridization with H1. In the presence of target survivin mRNA and DNA fuel strand, the target trigger the cascaded toehold-mediated strand displacement reaction which could occur and induce the association of plenty of Fc-tagged DNA strands on the sensor surface, then draws the Fc tags approach the gold electrode with a substantially increased redox current. To our knowledge, this is the first time to develop a proximity hybridization-regulated electrochemical sensor for mRNA detection via proximity-dependent surface HCR-based amplification strategies. Our method provided a novel electrochemical method for selective and ultrasensitive quantitative analysis of mRNA expression levels.

Compared with other electrochemical biosensor for DNA/RNA detection, our proposed sensing strategy has some remarkable advantages: (1) this is the first report using proximity-dependent surface HCR-based amplification strategies for highly sensitive target RNA detection; (2) the single-step homogeneous detection method avoids complicated labelling and washing procedures as required by other electrochemical biosensor; (3) the method is label-free, isothermal, non-enzymatic and easily applied to other DNA/RNA detection. Simple alteration of the DNA sequences may allow us to realize the determination of different kinds of DNA/RNA. These features can promise a great potential for amplified detection of various analytes and related biochemical research applications.

2. Experimental section

2.1. Chemicals and materials

All chemicals were of analytical-reagent grade without further purification. N-hydroxysulfosuccinimide (Sulfo-NHS), 1-ethyl-3-(3-dimethyl-aminopropyl) carbodiimide hydrochloride (EDC), tris(2-carboxyethyl) phosphine (TCEP), ferrocenecarboxylic acid (Fc) and 6-Mercaptohexanol (MCH) were purchased from Sigma-Aldrich Co., Ltd. (St. Louis, MO, USA). The HPLC-purified oligonucleotide sequences used in this work (sequences shown in Table S1) were synthesized by Takara Biotechnology Co. Ltd. (Dalian, China). All the other reagents were obtained from the Sinopharm Chemical Reagent Co., Ltd. (Shanghai, PRC). Ultrapure water (electric resistance >18.3 MΩ) was obtained through a Milli-Q water purification system (Millipore, Billerica, MA).

2.2. Labeling of Fc to NH_2-Modified oligonucleotides

The Fc label was conjugated to the 3′ NH_2-moiety of the oligonucleotide (probe H1), using the succinimide coupling (EDC-NHS) method [37]. Briefly, 100 μL of 10 μmol oligonucleotide (probe H1) was mixed with 100 μL of 10 mM PBS (pH 7.4) containing 10 mmol of ferrocenecarboxylic acid, 1 mM EDC, and 5 mM Sulfo-NHS, followed by incubation for 2 h at 37 °C. The conjugate was dialyzed against 10 mM PBS (500 mL) for 24 h to remove excessive ferrocenecarboxylic acid. The resulting solution was stored at −20 °C.

2.3. Gold electrode treatment and oligonucleotide immobilization

The electrodes pretreatment were according to the previous procedures [37]. The working gold electrodes, 99.99% (w/w) polycrystalline with a diameter of ~2 mm (CH Instruments, Inc.), were immersed in warm piranha solution (30% H_2O_2/concentrated H_2SO_4, 1:3 by volume) for 2 h three times and then washed with ultrapure water. Subsequently, the electrodes were polished on microcloth (Buehler) with a γ-alumina 0.05 μm suspension (CH Instruments, Inc.) for 3 min, followed by sonication in ultrapure water, ethanol and ultrapure water for 5 min in each. Finally, the electrode were again rinsed thoroughly with ultrapure water and dried in a nitrogen stream. The roughness factor of the electrode surface was estimated to be 1.6 ± 0.1 via determination of the gold electrode area using the gold oxide stripping peak area obtained in cyclic voltammetry (CV) measurements in 0.5 M H_2SO_4. The pretreated gold electrode was immersed in a solution containing 1.0 μM thiolated oligonuleotide in 10 mM PBS buffer (1.0 M NaCl and 10 mM TCEP, pH 7.4) for 12 h at room temperature. Thereafter, the electrode was immersed into 1 mM MCH for 20 min to remove the nonspecific DNA absorption. The electrode then was rinsed thoroughly with a 10 mM PBS buffer (pH 7.4) solution containing 0.5 M NaCl three times. Then the thiolated oligonucleotide immobilized electrode was stored at 4 °C in the PBS buffer solution. A FE20 digital pH meter with LE438 pH electrode (Mettler Toledo, Switzerland) was used to measure the pH value of the solutions.

2.4. Hybridization chain reaction (HCR)-Programmed surface hybridization

The DNA probes Fc-H1/H1 and H2 in 10 mM PBS buffer (pH 7.4) solution containing 0.3 M NaCl was heated to 90 °C for 10 min and then allowed to cool down to 37 °C for at least 3 h to form the double-strand DNA-duplex, respectively. The 20 μL mixture of 1 μM probe Fc-H1/H1, 1 μM probe H2, and specified concentration target RNA in 10 mM PBS

buffer (1 M NaCl, pH 7.4) were incubated on the thiolated oligonucleotide immobilized electrode for 3 h at 37 °C, followed by washing for 1 min in 40 mL of a 10 mM PBS buffer (pH 7.4) solution containing 0.5 M NaCl. Then the sensor was immersed in 50 mL of a 10 mM PBS buffer (pH 7.4) solution containing 0.5 M NaCl to be detected.

2.5. Gel electrophoresis

The dynamic assembly products were analyzed in 3% agarose hydrogel. The agarose gel electrophoresis was carried out in 1× TBE buffer at a constant voltage of 100 V for 90 min at room temperature, followed by staining using Goldview™ dye. The gels were scanned with a FR-980 gel image analysis system (Shanghai, China).

2.6. Atomic force Microscopy analysis

Samples were diluted in 1 TAE buffer containing 12.5 mM $MgCl_2$ and deposited on freshly cleaved mica (SPI, USA) for 3 min. Samples were rinsed with deionized water and dried with nitrgen. AFM imaging was performed in air in a tapping mode on a Bioscope system AFM (Brucker, USA). Silicon probes Tap 300Al-G (Budget Sensors, Bulgaria) with resonant frequency 300 kHz, force constant 40 N/m and tip radius 10 nm were used in the experiments. The image background was flattened by Nanoscope III a software.

2.7. RT-qPCR analysis of mRNA extracts from cells

Total RNA were extracted from MCF-10A, MCF-7, SK-BR-3 and Hela cells (10^6 cells) in triplicates using UNIQ-10 column Trizol total RNA purification kit (Sangon Biontech Co., Ltd, Shanghai, China). The integrity of total RNA was assessed by gel electrophoresis. The cDNA samples were prepared using AMV First Strand cDNA Synthesis Kit (BBI, Toronto, Canada) and were store at −20 °C for future use. qPCR analysis of mRNA was performed with SybrGreen PCR Master Mix (ABI, CA, USA) according to the manufacturer's instructions on an ABI StepOneplus qPCR instrument (CA, USA). Primers used for *survivin* mRNA were given as follows: the forward primer is 5′- TCC ACT GCC CCA CTG AGA AC -3′ and the reverse primer is 5′- TGG CTC CCA GCC TTC CA -3'. The copy numbers of *survivin* mRNA from these cell lines were calculated using a standard curve method.

2.8. Electrochemical characterization

All electrochemical measurements including differential pulse voltammetry (DPV), cyclic voltammetry (CV) and electrochemical impedance spectroscopy (EIS) were performed at room temperature using a three-electrode system that consists of a KCl saturated calomel reference electrode (SCE), a platinum counter electrode, and the gold working electrode. All electrochemical measurements were executed on an Autolab PGSTAT12/FRA2 potentiostat/galvanostat system (Eco Chemie, Utrecht, Netherlands). DPV was recorded in a 10 mM PBS buffer solution (0.5 M NaCl, pH 7.4) within the potential range from 0 V to 0.5 V (*vs* SCE) under a modulation amplitude of 25 mV and a scan rate of 10 mV/s with a step potential of 1 mV. CV was performed in a 10 mM PBS buffer (0.5 M NaCl, pH 7.4) solution within the potential range from −0.1 V to 0.5 V using a step potential of 0.01 V at the specified potential scan rate. EIS was performed in 50 mM PBS (pH 7.4) containing 5 mM Fe $(CN)_6^{3-}$/Fe$(CN)_6^{4-}$and 0.1 M KCl in the frequency range from 0.1 Hz to 100 kHz with 5 mV as the amplitude at a bias potential of 0.22 V (*vs* SCE). The reported DPV curves were background-subtracted using the GPES version 4.9.007 software (Eco Chemie, Ultrecht, Netherlands) through extrapolation to the baseline in the regions far from the peaks [38]. Before electrochemical measurements, the electrolyte solution received thorough treatment with high-purity nitrogen for 20 min, in order to avoid the interference by oxygen.

3. Results and discussion

3.1. Analytical principle of the electrochemical biosensor

Herein, the mRNA-fueled hybridization chain reaction is autonomously coupled with proximity-dependent surface hybridization for single-step, enzyme-free, and amplified electrochemical detection of target RNA, the principle of which is schematically illustrated in Scheme 1. The whole sensing strategy could be simply divided into two modules: the mRNA-fueled hybridization chain reaction and HCR-based post-amplification module. First, two hairpin-structured DNA probes H1 and H2 are designed, and H1 is labeled with a short ferrocene (Fc) tag at its 3′-end. The hybridization of mRNA target with the first toehold region of H1 yields a single stranded tail in H1, which then hybridizes with probe H2 and restores a single-strand tail in H2 with the same sequence of target. Thus, a hybridization chain reaction is subsequently triggered for alternating reactions between H1 and H2, producing a chain-like duplex assembly of H1 and H2 (Scheme 1). As a result, abundant 3′-end single-strand dangling tails were formed on the formed linear DNA concatamer, which can specifically hybridize with the oligonucleotides (thiolated probe) immobilized on a gold electrode surface, in a similar process to that of proximity ligation [31]. The double-stranded oligonucleotides display a flexible random-coil conformation that allows the Fc tags to approach the gold electrode and transfer the electrons efficiently, eventually resulting in significantly amplified electro-chemical signals for target RNA detection. By this way, the enzyme-free and label-free signal amplification could be easily achieved for target RNA detection.

3.2. Electrochemical characterization of fabricated mRNA biosensor

The developed electrochemical RNA biosensor was characterized with the Fc tags as an electrochemical indicator. The typical voltammetric characteristics of the sensor, in response to target RNA, are shown in Fig. 1. In the presence of a synthetic RNA target, a couple of strong redox peaks appeared at both 0.16 and 0.27 V (*vs* SCE) in CVs, characteristic of the electrochemistry of Fc on the electrode surface. Whereas in the absence of target RNA, there is almost no redox peaks observed (Fig. 1A). These observations disclosed that the sensor was sensitively responsive to the target RNA. Further observations were achieved in DPV measurements to examine the feasibility of the developed electrochemical biosensor for target RNA detection, as shown in Fig. 1B. The recorded DPV peak current could be attributed to the electrochemical reduction of Fc on the DNA modified electrodes, which was related with the peak I observed in Fig. 1A. In the absence of target RNA, the background electrochemical response could be only obtained (dashed line). However, it could be obviously seen that the sensor gave a remarkable increase peak (the standard deviation across 10 repetitive experiments was ~2.4%) at approximately 0.213 V (*vs* SCE) in the DPV curve in presence of target RNA and DNA fuel strands, and the peak currents increased notably by more than 20 times, compared with that in the case of no target RNA (the SD across 10 repetitive experiments was ~1.6%). Additionally, typical DPV curves revealed that there was only slightly increase of electrochemical response in the case of non-homologous RNA (a synthetic RNA with the most similar sequence to target RNA in human transcripts) control (dash-dot-dot line) [39], even at higher concentration, compared with the blank electrochemical response (dashed line), indicating the specificity of the electrochemical biosensors for target RNA. Also, the histogram for the electrochemical responses obtained at the control experiments is shown in Fig. 1C, in well consistent with the results of Fig. 1B. The hybridization chain reaction between H1 and H2 triggered by target RNA was also verified by agarose gel electrophoresis experiments (Fig. 1D). In the absence of RNA target, only the bands related to the H1 and H2 could be observed; while in the presence of target RNA, a series of DNA bands with high molecular weight over 100 bp were observed (lane e, Fig. 1D), suggesting the

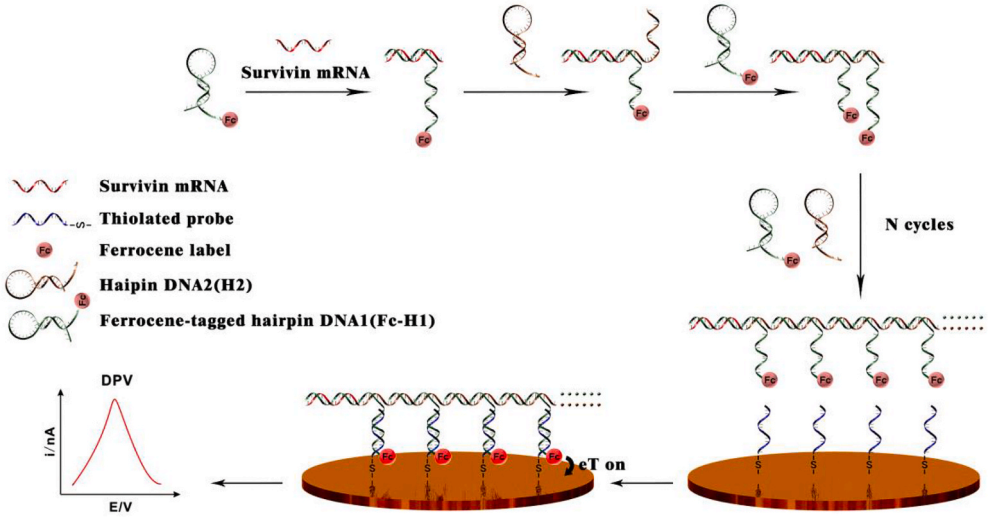

Scheme 1. Electrochemical sensing strategy of proximity-dependent surface hybridization chain reaction for mRNA detection.

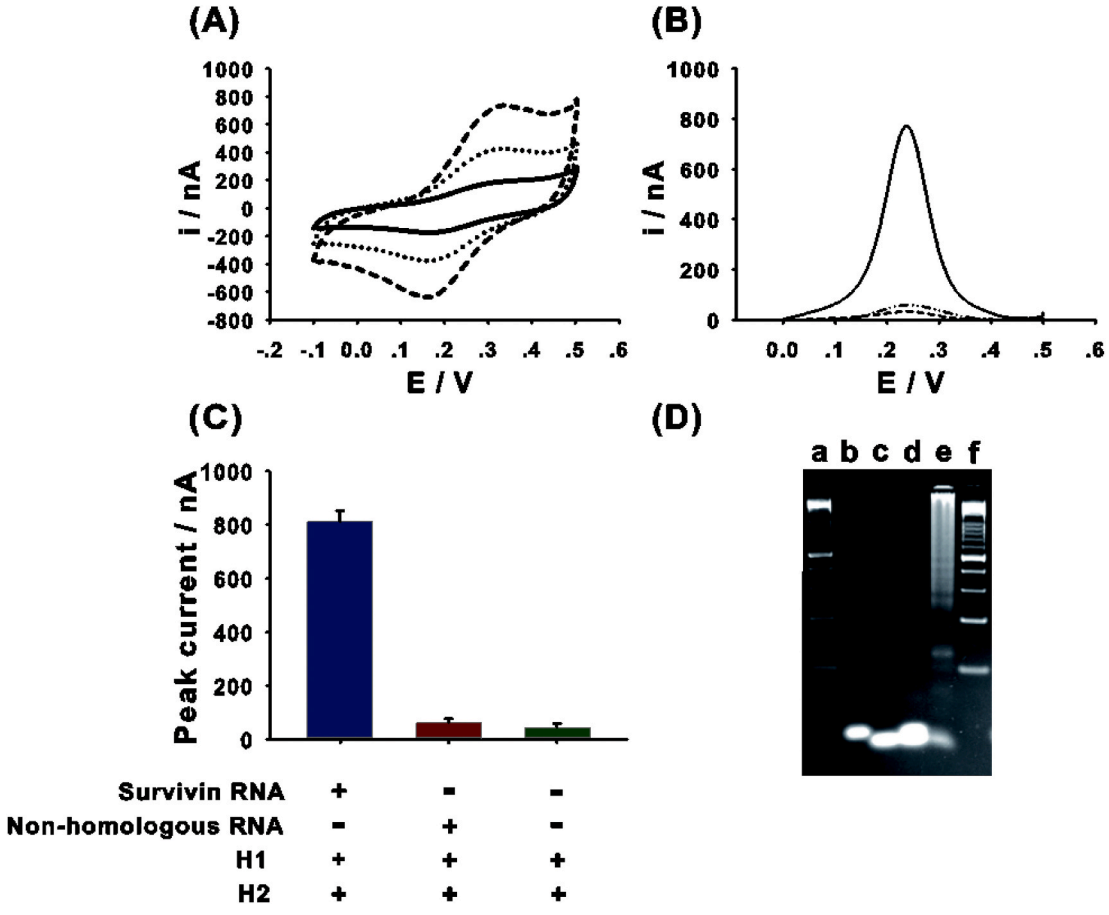

Fig. 1. (A) Typical CV curves of the sensor in response to Fc-H1 and H2 together with 0 M (solid line), 10 pM (dotted line), and 1 nM (dashed line) target RNA, respectively (scan rate = 100 mV/s). (B) Typical DPV curves of the sensor in response to Fc-H1 and H2 together with 1 nM target RNA (solid line), with 10 nM non-homologous RNA (dash-dot-dot line), or without target RNA (dashed line), respectively. (C) The bar chart of the DPV responses for the fabricated mRNA biosensor obtained at different experimental conditions. The experimental conditions were shown below the X-axis. (D) Electrophoresis image for HCR based assay in agarose gel: Lane a and Lane f, DNA size markers; Lane b, 1 μM probe H1; Lane c, 1 μM probe H2; Lane d, 1 μM probe H1 plus 1 μM probe H2; Lane e, triggered hybridization chain reaction between H1 and H2 in the presence of 100 nM RNA targets incubated for 3 h at 37 °C in 10 mM PBS buffer (1 M NaCl, pH 7.4).

occurrence of RNA-triggered hybridization chain reaction. Also, the average molecular weight of the product was inversely related to the amount of target, which was in consistent with the previous study. The dynamic assembly process for target-triggered HCR could be also easily monitored by current proximity-based surface hybridization strategy.

3.3. HCR-programmed surface hybridization

The synthesis of the nanoassembly was characterized by Atomic Force Microscope (AFM) (Fig. 2). After HCR-programmed surface hybridization, the DNA nanoassembly showed very thin nucleic acid coating on the surface of mica substrate.

3.4. EIS monitoring of the fabrication of the sensor

Electrochemical impedance spectra (EIS) is an effective tool for probing the features of surface-modified electrodes. Here, both the electrode modification and biosensor fabrication were confirmed by EIS measurements (Fig. 3). The EIS data were fitted by an equivalent electrical circuit (inset, Fig. 3). The components in the equivalent circuit included the solution resistance Rs, the charge-transfer resistance Rct, the constant phase element related to double layer capacitance (CPE), and the Warburg impedance (W, where W_S) Rw/(jw)1/2 and Rw is the diffusion resistance) [40]. Only a very small charge transfer resistance (Rct) value of about 498 Ω could be observed for the bare gold electrode (dash-dot-dot line, Fig. 3). The further MCH blocking made the Rct value with a further increase to be about 2581 Ω(dashed line in Fig. 3). In the presence of target RNA, the HCR proceeded with the association of H1 and H2 on the electrode surface. After HCR process on the electrode surface, the diameter of the semicircle increased evidently with a Rct value of about 8398 Ω (solid line in Fig. 3), indicating the formation of linear DNA concatamer repelling the negatively charged redox species more strongly. In contrast, no appreciable Rct value (about 3097 Ω, dotted line in Fig. 3) enhancement appeared in response to a non-homologous RNA. Moreover, the target RNA-triggered HCR proceeded with the association of Fc-H1 on the electrode surface, the obtained Rct value dropped to only 529 Ω (dash-dot line in Fig. 3), indicating an evident decrease of the Rct, which could be ascribed to the Fc approaching electrode surface by a proximity-dependent surface hybridization strategy for constructing an efficient signal-on electrochemical sensing system. The EIS experiments could further provide beneficial supports for the biosensor fabrication process by the mRNA-fueled HCR-based amplification strategy.

3.5. Detection performance of the biosensor

To study the controlled factor of the electrochemical process on the electrode surface, the effect of scan rates on the CV peak currents was investigated. As shown in Fig. 4A, in the absence of target RNA, the reduction peak currents of the sensor were observed to increase in linear correlation to the scan rate in the range of 10–120 mV/s. A linear dependency of the reduction peak currents on the scan rates was also obtained for the sensor in the presence of target RNA, as shown in Fig. 4B.

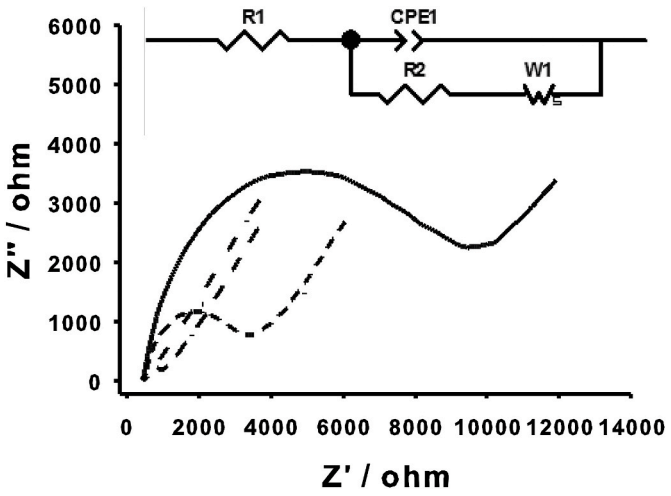

Fig. 3. Nyquist plot (Z_{im} vs Z_{re}) for EIS of the different modified electrodes. The curves were obtained for bare gold electrode (dash-dot-dot line), the thiolated probe-modified electrode (dashed line), the modified electrode after HCR used Fc-unlabeled H1 in the present of 1 nM target RNA (solid line), the modified electrode after HCR used Fc-labeled H1 in the present of 1 nM target RNA (dash-dot line), and the modified electrode in the absence of 10 nM non-homologous RNA (dotted line). (Inset shows the equivalent circuit).

These observations manifested that the sensor demonstrated typical surface-bound electrochemical processes and the Fc tags were confined to the electrode surface. The sensitivity of the proposed biosensor to detect target mRNA was further evaluated by measuring different concentrations of target mRNA (Fig. 5). The DPV method was used here for its low background current effect, and was performed in 10 mM PBS buffer solution (0.5 M NaCl, pH 7.4) after the incubation of recognized electrodes into 50 pM Fc for 20 min. The DPV peak current was obtained to reflect the relevant information about the electrostatic adsorption of Fc, and further DNA assemblies on the electrode surface after mRNA recognition and signal amplification. As shown in Fig. 5A, the DPV peak increased continually with the increase of the target mRNA concentration. As shown in Fig. 5B, the calibration curve between the electrochemical intensity and the logarithm value (inset) of the mRNA target concentration. As proposed, electrochemical response would be more easily achieved at a relatively low concentration of target RNA owing to the target-triggered formation of the self-assembled polymerization of two species of H-DNA for the promotion of proximity-based surface hybridization. A good linear relationship was obtained for the DPV peak to the logarithm value (inset) of target mRNA concentration in the range of 10 fM to 1 nM. The detection limit, defined as four times the standard

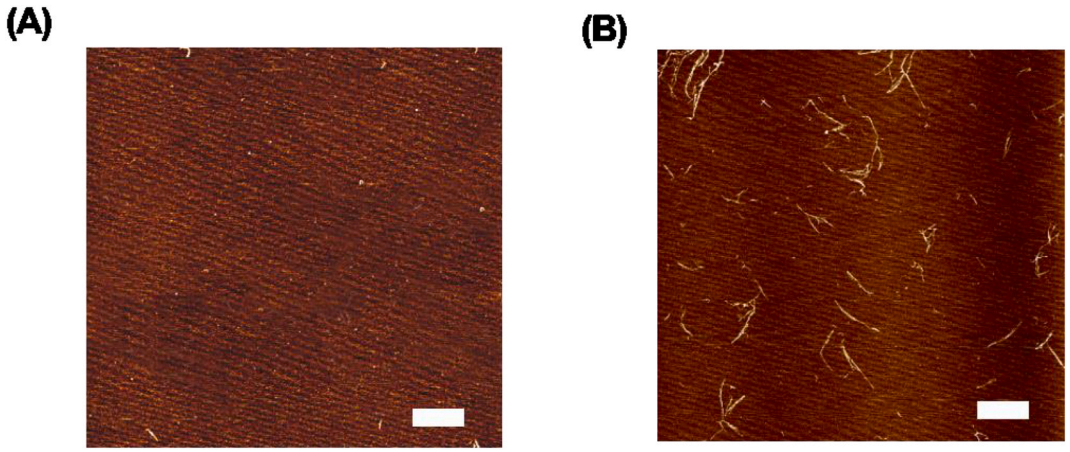

Fig. 2. AFM images for DNA nanoassembly on a mica substrate before (A) and after (B) HCR-programmed surface hybridization. Scan bars are 1 μm.

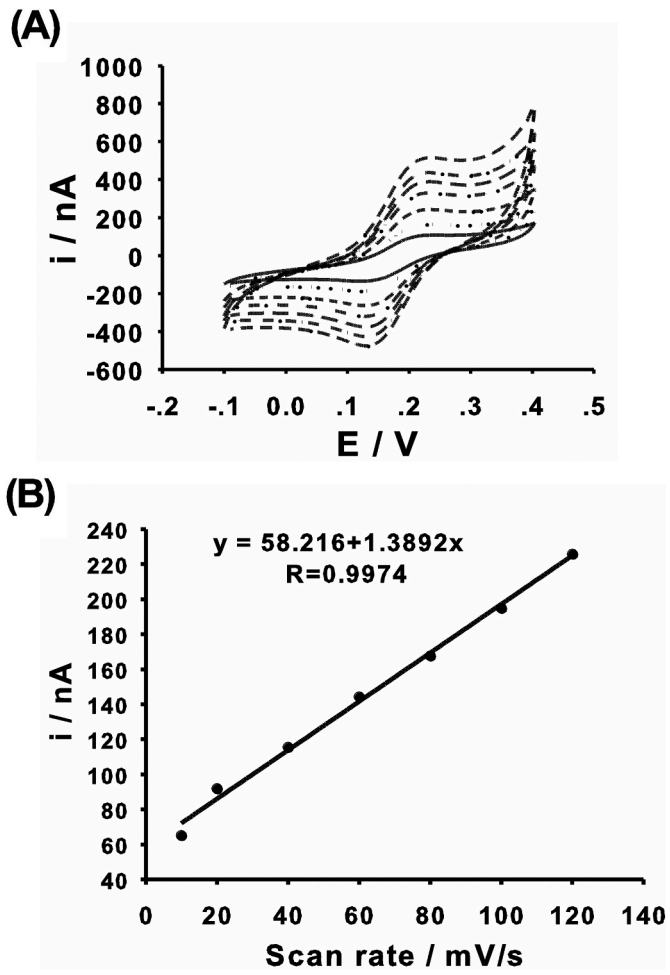

Fig. 4. (A) CV curves of the sensor in response to 10 pM RNA at varying potential scanning rates of 10, 20, 40, 60, 80, 100, and 120 mV/s. (B) Plot of the oxidation peak currents versus scan rates.

deviation of the background, was about 3 fM, which was superior or comparable to most of the reported electrochemical DNA biosensors (Table S2) and is sensitive enough to detect those variabilities between multiple cell lines. It seems that the HCR-programmed proximity-based surface hybridization strategy shows a more favorable prospect for the point-of-care applications, owing to its easier to operate, cost-effective, and sensitivity enough.

3.6. Selectivity of the biosensor

We further designed a series of single-base mismatched DNA sequences (sequences shown in Table S1) and investigated the specificity of the developed biosensor for detecting target RNA (Fig. 6). Most mismatched DNA only showed electrochemical responses close to the background signal at the same concentration, indicating a good performance of the biosensor to discriminate target mRNA and mismatched nucleic acid. All the electrochemical responses toward the mismatched nucleic acid sequences were less than 25% of that toward perfect target mRNA. Additionally, the selectivity of the fabricated electrochemical mRNA biosensor for detecting target mRNA from different biological samples was also checked by using *survivin* mRNA extracted from multiple cell lines including Hela, MCF-7, MCF-10A and SK-BR-3 cells, and so on (Fig.S1-3, and Fig. 7). It could be seen that extracts from distinct cell lines yielded no obvious interference toward the detection of target mRNA, suggesting the potential of the fabricated electrochemical biosensor for the detection of target mRNA in different biological

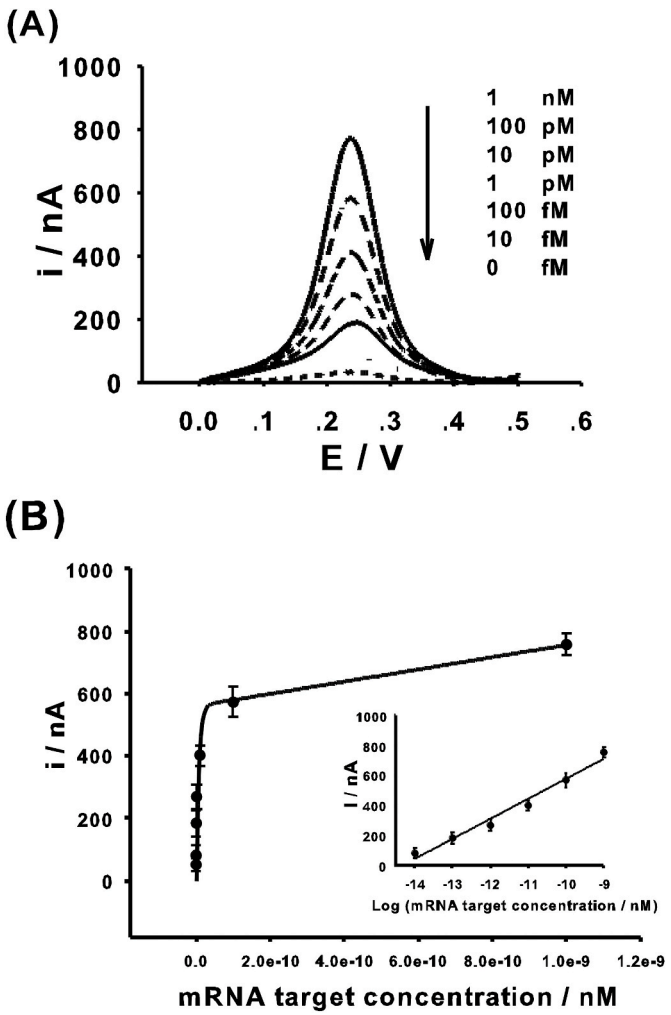

Fig. 5. (A) Typical DPV curves of the sensor in response to target RNA of varying concentrations (0 M, 10 fM, 100 fM, 1 pM, 10 pM, 100 pM, and 1 nM). (B) Plot of DPV peak currents versus mRNA target concentrations. Inset: DPV peak currents versus logarithmic mRNA target concentrations. Error bars are standard deviation across four repetitive experiments using four different electrodes.

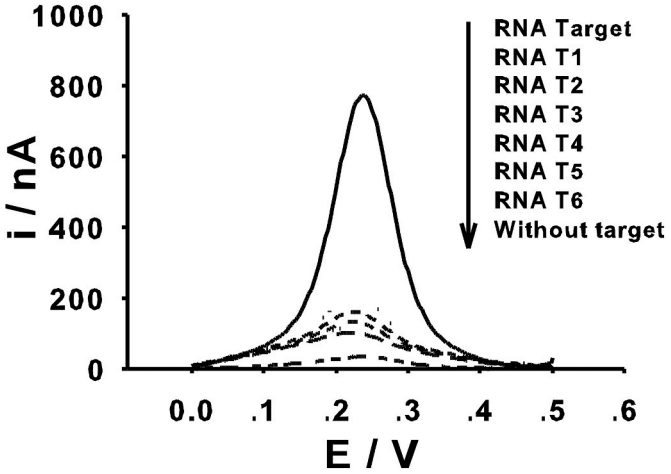

Fig. 6. Specificity evaluation of electrochemical strategy for detecting 1 nM RNA target and 10 fold (10 nM) single-base mismatched RNA (T1, T2, T3, T4, T5 and T6), respectively.

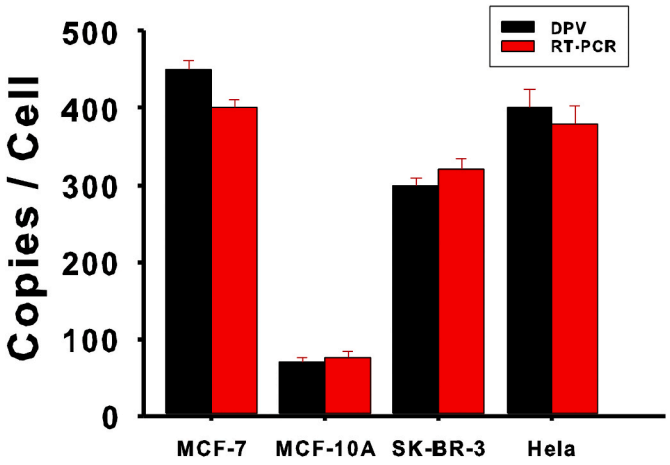

Fig. 7. Estimated copies of *survivin* mRNA in total RNA from MCF-7, MCF-10A, SK-BR-3 and Hela cells by the developed electrochemical method and RT-PCR, respectively. Error bars are standard deviations of four repetitive experiments using four different electrodes.

samples. Four independent experiments demonstrated that the developed biosensor could retain high detection efficiency toward target mRNA similar to that obtained from qPCR experiments, with less labor and easier manipulating, indicating a relatively robust stability of the proposed biosensor.

4. Conclusions

In summary, we have proposed a novel enzyme-free electrochemical biosensor by integrating surface-proximity ligation with HCR amplification reaction for ultrasensitive mRNA detection. Compared with traditional electrochemical analysis, our proposed sensing strategy exhibit both stringent recognition and efficient signal amplification of the target, with some inherent advantages: 1) by taking advantage of the target mRNA initiates a hybridization cascade between two hairpin sequences through toehold mediated strand displacement, highly specific enzyme-free recognition of dynamics assembly is achieved; 2) with the help of two hairpin DNA probes, autonomous execution of proximity-based surface hybridization makes it possible to realize the recognition and amplification processes quickly, which could greatly minimize the operational difficulty; and 3) most importantly, such proximity-dependent surface HCR induce the association of plenty of Fc-tagged DNA strands on the sensor surface, which draws Fc tags onto the electrode's surface with a substantially stable redox current, which could reduce non-specific protein adsorption and improve detection sensitivity. Thus, this electrical biosensor would be beneficial for the target biorecognition and measurement, providing a competitive candidate technique for studying expression and dynamic assembly in cells and tissues by a combination of biomolecular reactions and electrodes. Additionally, this work could inspire the integration of various nucleic-acid amplification into diverse selective assays to detect low-concentration biomolecules in cells or tissues for clinical use with low cost.

Credit author statement

Yu-Hong Cheng, Methodology, Validation, Formal analysis, Investigation, Writing original draft. Si-Jia Liu, Conceptualization, Writing original draft, Writing -review & editing, Project administration, Funding acquisition. Jian-Hui Jiang, Conceptualization, Formal analysis, Writing original draft, Writing review & editing, Supervision, Project administration, Funding acquisition.

Declaration of competing interest

The authors declare that they have no known competing financial interests or personal relationships that could have appeared to influence the work reported in this paper.

Acknowledgements

This work was financially supported by the Natural Science Foundation of China (No. 21527810, 81860256, 21505041), China Postdoctoral Science Foundation funded project (No.2017M613270XB), and Guangxi Natural Science Foundation (No. 2017GXNSFAA198099, AD17195079).

Appendix A. Supplementary data

Supplementary data to this article can be found online at https://doi.org/10.1016/j.talanta.2020.121536.

References

[1] C.E. Holt, S.L. Bullock, Subcellular mRNA localization in animal cells and why it matters, Science 326 (2009) 1212–1216, https://doi.org/10.1126/science.1176488.
[2] A. Jayagopal, K.C. Halfpenny, J.W. Perez, D.W. Wright, Hairpin DNA-functionalized gold colloids for the imaging of mRNA in live cells, J. Am. Chem. Soc. 132 (2010) 9789–9796, https://doi.org/10.1021/ja102585v.
[3] S. Apostolaki, M. Perraki, G. Kallergi, M. Kafousi, S. Papadopoulos, A. Kotsakis, A. Pallis, N. Xenidis, L. Kalmanti, K. Kalbakis, S. Agelaki, A. Kalykaki, C. Stournaras, E. Stathopoulos, V. Georgoulias, D. Mavroudis, Detection of occult HER2 mRNA-positive tumor cells in the peripheral blood of patients with operable breast cancer: evaluation of their prognostic relevance, Breast Canc. Res. Treat. 117 (2009) 525–534, https://doi.org/10.1007/s10549-008-0239-3.
[4] S.R. Morris, L.A. Carey, Gene expression profiling in breast cancer, Curr. Opin. Oncol. 19 (2007) 547–551, https://doi.org/10.1097/CCO.0b013e3282f0ada3.
[5] F. Li, E.S. Barnathan, K. Karik'o, Rapid method for screening and cloning cDNAs generated in differential mRNA display: application of Northern blot for affinity capturing of cDNAs, Nucleic Acids Res. 22 (1994) 1764–1765, https://doi.org/10.1093/nar/22.9.1764.
[6] P.M. Chan, T. Yuen, F. Ruf, J. Gonzalez-Maeso, S.C. Sealfon, Method for multiplex cellular detection of mRNAs using quantum dot fluorescent in situ hybridization, Nucleic Acids Res. 33 (2005) e161, https://doi.org/10.1093/nar/gni162.
[7] W.S. Choi, C.A. Machida, O.K. Ronnekleiv, Distribution of dopamine D1, D2, and D5 receptor mRNAs in the monkey brain: ribonuclease protection assay analysis, Mol. Brain Res. 31 (1995) 86–94, https://doi.org/10.1016/0169-328x(95)00038-t.
[8] M.O. Noordewier, P.V. Warren, Gene expression microarrays and the integration of biological knowledge, Trends Biotechnol. 19 (2001) 412–415, https://doi.org/10.1016/S0167-7799(01)01735-8.
[9] A. Schulze, J. Downward, Navigating gene expression using microarrays — a technology review, Nat. Cell Biol. 3 (2001) 190–195, https://doi.org/10.1038/35087138.
[10] T. Nolan, R.E. Hands, S.A. Bustin, Quantification of mRNA using real-time RT-PCR, Nat. Protoc. 1 (2006) 1559–1582, https://doi.org/10.1038/nprot.2006.236.
[11] A. Peixoto, M. Monteiro, B. Rocha, H. Veiga-Fernandes, Quantification of multiple gene expression in individual cells, Genome Res. 14 (2004) 1938–1947, https://doi.org/10.1101/gr.2890204.
[12] X.B. Zhong, P.M. Lizardi, X.H. Huang, P.L. Bray-Ward, D.C. Ward, Visualization of oligonucleotide probes and point mutations in interphase nuclei and DNA fibers using rolling circle DNA amplification, Proc. Natl. Acad. Sci. U.S.A. 98 (2001) 3940–3945, https://doi.org/10.1073/pnas.061026198.
[13] W. Zhao, M.M. Ali, M.A. Brook, Y. Li, Rolling circle amplification: applications in nanotechnology and biodetection with functional nucleic acids, Angew. Chem. Int. Ed. 47 (2008) 6330–6337, https://doi.org/10.1002/anie.200705982.
[14] R. Deng, L. Tang, Q. Tian, Y. Wang, L. Lin, J. Li, Toehold-initiated rolling circle amplification for visualizing individual MicroRNAs in situ in single cells, Angew. Chem. Int. Ed. 126 (2014) 2421–2425, https://doi.org/10.1002/anie.201309388.
[15] Q. Xu, A. Cao, L. Zhang, C. Zhang, Rapid and label-free monitoring of exonuclease III-assisted target recycling amplification, Anal. Chem. 84 (2012) 10845–10851, https://doi.org/10.1021/ac303095z.
[16] S. Liu, C. Wang, C. Zhang, Y. Wang, B. Tang, Label-free and ultrasensitive electrochemical detection of nucleic acids based on autocatalytic and exonuclease III-assisted target recycling strategy, Anal. Chem. 85 (2013) 2282–2288, https://doi.org/10.1021/ac303225p.
[17] C. Tao, Y. Yan, H. Xiang, D. Zhu, W. Cheng, H. Ju, S. Ding, A new mode for highly sensitive and specific detection of DNA based on exonuclease III-assisted target recycling amplification and mismatched catalytic hairpin assembly, Chem. Commun. 51 (2015) 4220–4222, https://doi.org/10.1039/c5cc00385g.
[18] Y. Chen, B. Jiang, Y. Xiang, Y. Chai, R. Yuan, Target recycling amplification for sensitive and label-free impedimetric genosensing based on hairpin DNA and

graphene/Au nanocomposites, Chem. Commun. 47 (2011) 12798–12800, https://doi.org/10.1039/c1cc14902d.
[19] J.M. Lage, J.H. Leamon, T. Pejovic, S. Hamann, M. Lacey, D. Dillon, R. Segraves, B. Vossbrinck, A. González, D. Pinkel, D.G. Albertson, J. Costa, P.M. Lizardi, Whole genome analysis of genetic alterations in small DNA samples using hyperbranched strand displacement amplification and Array−CGH, Genome Res. 13 (2003) 294–307, https://doi.org/10.1101/gr.377203.
[20] J. Liu, Z. Cao, Y. Lu, Functional nucleic acid sensors, Chem. Rev. 109 (2009) 1948–1998, https://doi.org/10.1021/cr030183i.
[21] J.L. He, Z.S. Wu, H. Zhou, H.Q. Wang, J.H. Jiang, G.L. Shen, R.Q. Yu, Fluorescence aptameric sensor for strand displacement amplification detection of cocaine, Anal. Chem. 82 (2010) 1358–1364, https://doi.org/10.1021/ac902416u.
[22] R.M. Dirks, N.A. Pierce, Triggered amplification by hybridization chain reaction, Proc. Natl. Acad. Sci. U.S.A. 101 (2004) 15275–15278, https://doi.org/10.1073/pnas.0407024101.
[23] Y. Chen, J. Xu, J. Su, Y. Xiang, R. Yuan, Y. Chai, *In situ* hybridization chain reaction amplification for universal and highly sensitive electrochemiluminescent detection of DNA, Anal. Chem. 84 (2012) 7750–7755, https://doi.org/10.1021/ac3012285.
[24] Z. Ge, M. Lin, P. Wang, H. Pei, J. Yan, J. Shi, Q. Huang, D. He, C. Fan, X. Zuo, Hybridization chain reaction amplification of MicroRNA detection with a tetrahedral DNA nanostructure-based electrochemical biosensor, Anal. Chem. 86 (2014) 2124–2130, https://doi.org/10.1021/ac4037262.
[25] G. Zhou, M. Lin, P. Song, X. Chen, J. Chao, L. Wang, Q. Huang, W. Huang, C. Fan, X. Zuo, Multivalent capture and detection of cancer cells with DNA nanostructured biosensors and multi-branched hybridization chain reaction amplification, Anal. Chem. 86 (2014) 7843–7848, https://doi.org/10.1021/ac502276w.
[26] C. Jung, A.D. Ellington, Diagnostic applications of nucleic acid circuits, Acc. Chem. Res. 47 (2014) 1825–1835, https://doi.org/10.1021/ar500059c.
[27] J. Zhao, S. Hu, Y. Cao, B. Zhang, G. Li, Electrochemical detection of protein based on hybridization chain reaction-assisted formation of copper nanoparticles, Biosens. Bioelectron. 66 (2015) 327–331, https://doi.org/10.1016/j.bios.2014.11.039.
[28] Y. Zhang, Z. Chen, Y. Tao, Z. Wang, J. Ren, X. Qu, Hybridization chain reaction engineered dsDNA for Cu metallization: an enzyme-free platform for amplified detection of cancer cells and microRNAs, Chem. Commun. 51 (2015) 11496–11499, https://doi.org/10.1039/c5cc03144c.
[29] J. Huang, H. Wang, X. Yang, K. Quan, Y. Yang, L. Ying, N. Xie, M. Ou, K. Wang, Fluorescence resonance energy transfer-based hybridization chain reaction for in situ visualization of tumor-related mRNA, Chem. Sci. 7 (2016) 3829–3835, https://doi.org/10.1039/c6sc00377j.
[30] L. Jia, S. Shi, R. Ma, W. Jia, H. Wang, Highly sensitive electrochemical biosensor based on nonlinear hybridization chain reaction for DNA detection, Biosens. Bioelectron. 80 (2016) 392–397, https://doi.org/10.1016/j.bios.2016.02.007.
[31] Y.L. Zhang, Y. Huang, J.H. Jiang, G.L. Shen, R.Q. Yu, Electrochemical aptasensor based on proximity-dependent surface hybridization assay for single-step, reusable, sensitive protein detection, J. Am. Chem. Soc. 129 (2007) 15448–15449, https://doi.org/10.1021/ja0773047.
[32] J. Yang, Y. Wu, C. Gan, R. Yuan, Y. Xiang, Target-programmed and autonomous proximity binding aptasensor for amplified electronic detection of thrombin, Biosens. Bioelectron. 117 (2018) 743–747, https://doi.org/10.1016/j.bios.2018.06.069.
[33] A. Anne, A. Bouchardon, J. Moiroux, 3′-Ferrocene-Labeled oligonucleotide chains end-tethered to gold electrode surfaces: novel model systems for exploring flexibility of short DNA using cyclic voltammetry, J. Am. Chem. Soc. 125 (2003) 1112–1113, https://doi.org/10.1021/ja028640k.
[34] D.A. Di Giusto, W.A. Wlassoff, J.J. Gooding, B.A. Messerle, G.C. King, Proximity extension of circular DNA aptamers with real-time protein detection, Nucleic Acids Res. 33 (2005) e64, https://doi.org/10.1093/nar/gni063.
[35] H. Zhang, F. Li, B. Dever, C. Wang, X.F. Li, X.C. Le, Assembling DNA through affinity binding to achieve ultrasensitive protein detection, Angew. Chem. Int. Ed. 52 (2013) 10698–10705, https://doi.org/10.1002/anie.201210022.
[36] F. Li, H. Zhang, Z. Wang, X. Li, X.F. Li, X.C. Le, Dynamic DNA assemblies mediated by binding-induced DNA strand displacement, J. Am. Chem. Soc. 135 (2013) 2443–2446, https://doi.org/10.1021/ja311990w.
[37] S.J. Liu, H.G. Nie, J.H. Jiang, G.L. Shen, R.Q. Yu, Electrochemical sensor for mercury (II) based on conformational switch mediated by interstrand cooperative coordination, Anal. Chem. 81 (2009) 5724–5730, https://doi.org/10.1021/ac900527f.
[38] J. Hirst, J.L.C. Duff, G.N.L. Jameson, M.A. Kemper, B.K. Burgess, F.A. Armstrong, Kinetics and mechanism of redox-coupled, long-range proton transfer in an iron-sulfur protein. Investigation by fast-scan protein-film voltammetry, J. Am. Chem. Soc. 120 (1998) 7085–7094, https://doi.org/10.1021/ja980380c.
[39] http://blast.ncbi.nlm.nih.gov/.
[40] F. Patolsky, A. Lichtenstein, I. Willner, Electronic transduction of DNA sensing processes on surfaces: amplification of DNA detection and analysis of single-base mismatches by tagged liposomes, J. Am. Chem. Soc. 123 (2001) 5194–5205, https://doi.org/10.1021/ja0036256.